

Metabolic Engineering of *Acinetobacter baylyi* ADP1 for Improved Growth on Gluconate and Glucose

Matti Kannisto, Tommi Aho, Matti Karp, Ville Santala

Department of Chemistry and Bioengineering, Tampere University of Technology, Tampere, Finland

A high growth rate in bacterial cultures is usually achieved by optimizing growth conditions, but metabolism of the bacterium limits the maximal growth rate attainable on the carbon source used. This limitation can be circumvented by engineering the metabolism of the bacterium. *Acinetobacter baylyi* has become a model organism for studies of bacterial metabolism and metabolic engineering due to its wide substrate spectrum and easy-to-engineer genome. It produces naturally storage lipids, such as wax esters, and has a unique gluconate catabolism as it lacks a gene for pyruvate kinase. We engineered the central metabolism of *A. baylyi* ADP1 more favorable for gluconate catabolism by expressing the pyruvate kinase gene (*pykF*) of *Escherichia coli*. This modification increased growth rate when cultivated on gluconate or glucose as a sole carbon source in a batch cultivation. The engineered cells reached stationary phase on these carbon sources approximately twice as fast as control cells carrying an empty plasmid and produced similar amount of biomass. Furthermore, when grown on either gluconate or glucose, *pykF* expression did not lead to significant accumulation of overflow metabolites and consumption of the substrate remained unaltered. Increased growth rate on glucose was not accompanied with decreased wax ester production, and the *pykF*-expressing cells accumulated significantly more of these storage lipids with respect to cultivation time.

Bacterial growth rate has traditionally been improved by modifying cultivation conditions, such as temperature, pH, and nutrient concentrations. Some carbon sources allow a higher growth rate than others (1). For example, *Escherichia coli* grows generally better on glycolytic carbon sources than on gluconeogenic ones. This preference cannot be altered by modification of growth conditions, and if the organism is to be efficiently cultivated using some nonpreferred carbon source, its metabolism has to be modified to allow this. The growth rate of *E. coli* on two gluconeogenic substrates, pyruvate and succinate, has been successfully increased by overexpressing its genes for phosphoenolpyruvate synthase or phosphoenolpyruvate carboxykinase, respectively (2). The growth rate and growth yield of *Gluconobacter oxydans* on glucose have been improved by knocking out its genes for gluconate formation (3). Less attention has been paid to enhancing the growth by expressing foreign genes.

Acinetobacter baylyi ADP1 (4), previously known as *Acinetobacter calcoaceticus* BD413 or LMD 82.3, is a Gram-negative and nonmotile coccus that is known for its catabolic capabilities and the ease with which it can be genetically transformed (5). It is a soil bacterium and can grow on various carbon sources (6) from which aromatic compounds' catabolism is probably the best characterized (5, 7). Its genetics and metabolism have also been studied extensively (8). These traits make it an attractive host organism for various biotechnological applications (9). The suitability of *A. baylyi* has been studied, for example, in production of cyanophycin (10), emulsan (11), and storage lipids (12). *A. baylyi* has also been used in D-xylulose production from D-xylose, where the cells were used in oxidation of residual D-xylose to D-xylonic acid (13).

While *A. baylyi* ADP1 generally grows well on carbon sources that enter main metabolic pathways through citric acid cycle, its growth on glucose is rather slow. It catabolizes glucose with an Entner-Doudoroff pathway (Fig. 1), where one molecule of glucose is converted to one molecule of pyruvate and one molecule of glyceraldehyde-3-phosphate. While the former can be funneled directly into citric acid cycle, the latter has to be converted to

phosphoenolpyruvate, carboxylated to oxaloacetate, converted to malate, and then decarboxylated to pyruvate (14), if it is to be completely oxidized to CO₂. This is necessary since *A. baylyi* ADP1 lacks the gene for one of the phosphoenolpyruvate-pyruvate-oxaloacetate node's common enzymes, pyruvate kinase (15). It has been shown that its parental strain, which lacks this enzymatic activity, uses majority of the glyceraldehyde-3-phosphate produced in glucose catabolism for biosynthetic purposes (15). Thus, it seems that by increasing the flux from glycolysis to citric acid cycle it might be possible to affect growth characteristics of the organism. *E. coli*'s phosphoenolpyruvate-pyruvate-oxaloacetate node has been studied extensively (16) and has been subjected to metabolic engineering (17). For example, overexpression of its gene for phosphoenolpyruvate carboxylase reduced acetate formation when cultivated on glucose (18). To the best of our knowledge, *A. baylyi*'s phosphoenolpyruvate-pyruvate-oxaloacetate node has not been subjected to extensive modifications. Elbahloul and Steinbüchel have overexpressed *A. baylyi* ADP1's gene for phosphoenolpyruvate carboxylase in an attempt to increase its cyanophycin production but did not report any change in growth rate when grown on gluconate as a carbon source (10). Here, we engineered *A. baylyi* ADP1 to express *E. coli*'s gene for pyruvate kinase, *pykF*, and characterized its growth on gluconate and glucose.

Received 17 June 2014 Accepted 29 August 2014

Published ahead of print 5 September 2014

Editor: S.-J. Liu

Address correspondence to Matti Kannisto, matti.kannisto@tut.fi.

Copyright © 2014, American Society for Microbiology. All Rights Reserved.

doi:10.1128/AEM.01837-14

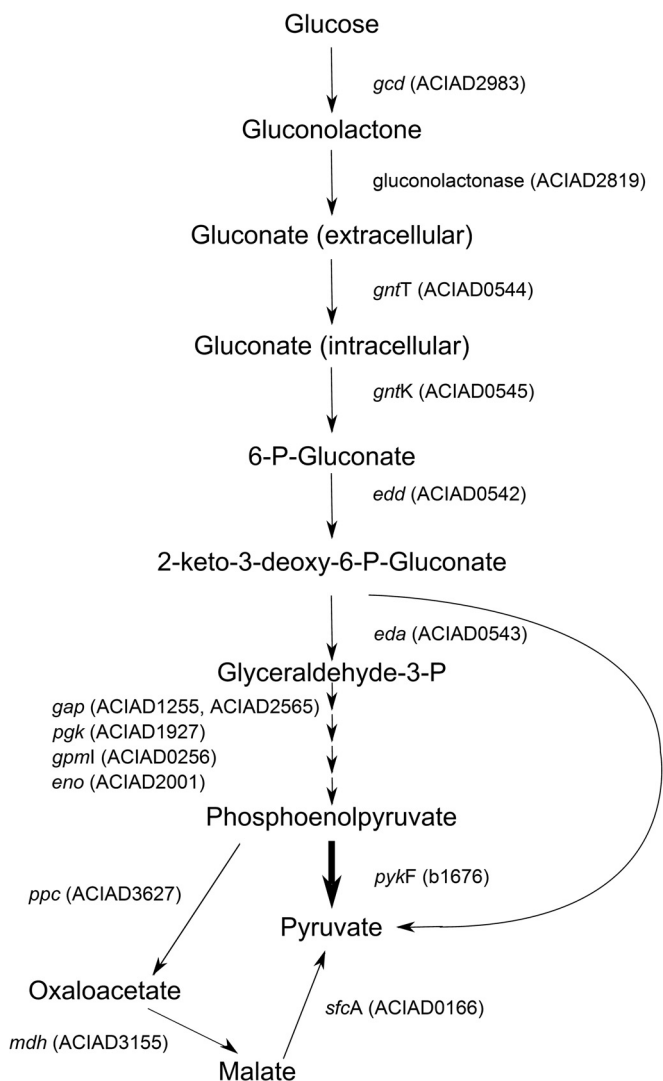


FIG 1 Simplified representation of catabolism of glucose to pyruvate by *A. baylyi* ADP1. Thin arrows indicate reactions that occur in the wild-type cell, and the thick arrow indicates a reaction catalyzed by a pyruvate kinase for which the wild-type cell does not have a gene for. (Adapted from Young et al. [5] and Taylor and Juni [15].)

MATERIALS AND METHODS

Bacterial strains and construction of the plasmids. Wild-type *A. baylyi* ADP1 (DSM 24193) was used as a host for the *pykF* expression plasmid. Wild-type cells or cells with an empty plasmid were used as a control strain. Construction of the plasmids was carried out in *E. coli* XL1-Blue, and genetic engineering was performed according to well-established methods (19). *pykF* was cloned with the primers 5'-GTTTCTTCGAATTCGCGGCCGCTTCTAGATGAAAAAGACCAAATTTGTTTCACC-3' and 5'-GTTTCTTCCTGCAGCGGCCGCTACTAGTATTACAGGACGTGAACAGATGC-3' using the genomic DNA of *E. coli* K-12 MG1655 as a template. The 1.5-kb fragment was digested with EcoRI and SpeI and ligated with pBAVIC-pBAD, which had been digested with the same pair of enzymes. pBAVIC-pBAD plasmid used here is the one used by Santala et al. (20) but to which the arabinose promoter had been cloned with the primers 5'-GTTTCTTCGAATTCGCGGCCGCTTCTAGAGCAATTCGGATAAAAGCGGATTC-3' and 5'-GTTTCTTCCTGCAGCGGCCGCTACTAGTAATTCCTCCTGTTAGCCCAAAAAAC-3'. The control plasmid was produced by digesting pBAVIC-pBAD with XbaI and SpeI

and ligating the pBAVIC backbone with itself. The plasmids were transformed into *E. coli*, and the insert was verified with sequencing. Natural transformation of the wild-type *A. baylyi* ADP1 with the plasmids was carried out essentially as described by Metzgar et al. (21). The presence of the plasmid in the chloramphenicol-resistant colonies, picked from an agar plate with 25 mg/liter of the antibiotic, was verified by digesting the purified plasmid with EcoRI and SpeI and subjecting the digested plasmid to agarose gel electrophoresis analysis. The cells carrying the plasmid with a correct insert size were used in cultivation experiments.

Growth medium and cultivation conditions. Cultivation experiments were carried out in a medium containing the following components: 6.7 g/liter $K_2HPO_4 \cdot 3H_2O$, 3.4 g/liter KH_2PO_4 , 0.3 g/liter $MgSO_4$, 22.2 mg/liter $CaCl_2$, 4.2 mg/liter $FeCl_3$, and 1.0 g/liter NH_4Cl . Sodium-D-gluconate, D-glucose, and L-arabinose were used at the concentrations indicated in Results. All cultivation experiments were carried out in 50 ml of the medium at 30°C with a shaking speed of 300 rpm. Main cultivations were started by inoculating to an optical density at 600 nm (OD_{600}) of <0.1.

Measurement of growth and analysis of metabolites. OD_{600} measurements were used to determine the growth rates of the cells. The measurements were taken once an hour, and the first data point was 2 h from the beginning of each cultivation. Slopes of the $\ln(OD_{600})$ versus time (in hours) were used to determine the growth rate in the exponential phase (μ). Linear regression slopes were calculated from parts of the graph that consisted of six data points (3 to 8 h after the beginning of the cultivation) for gluconate cultivation and five data points (8 to 16 h after the beginning of the cultivation) for glucose cultivation, and generally good R^2 values (>0.97) were obtained. Doubling times of the cells were calculated by dividing $\ln 2$ by the growth rates.

Concentrations of D-gluconate, D-glucose, lactate, glycerol, acetate, ethanol, and butyrate were determined with high-performance liquid chromatography (HPLC). HPLC was carried out using the same equipment and operation condition as those used by Santala et al. (12), except for the column, which was a Rezex RHM-Monosaccharide H+ (8%) column (Phenomenex, Torrance, CA). Standards (0.05 to 10 mM) were prepared in sterile ion-exchanged water and were run in duplicates. The samples were diluted in ratio of 1:10 with sterile ion-exchanged water prior to HPLC analysis.

Lipids for thin-layer chromatography (TLC) analysis were extracted by centrifuging the cells for 10 min at $20,000 \times g$ and resuspending the pellet in 0.5 ml of methanol. Next, 0.25 ml of $CHCl_3$ and 0.1 ml of phosphate-buffered saline (PBS) were added to the suspensions, and the samples were mixed gently for an hour. The samples were centrifuged for 5 min at $20,000 \times g$, and then 0.25 ml of $CHCl_3$ and 0.25 ml of PBS were added, after which the samples were mixed gently overnight. The samples were centrifuged again for 5 min at $20,000 \times g$, and the lowest phases were used in TLC analysis, which was carried out as described previously (22). Wax esters were visualized with iodine staining. TLC picture colors were modified using Microsoft Office 2010 Picture Manager so that color saturation was decreased to 0% and contrast was increased to 100%.

Determination of pyruvate kinase activity. The pyruvate kinase activity assay was performed essentially as described previously by Netzer et al. (23). Cells were collected from the cultivations in the exponential growth phase by centrifugation for 5 min at $25,000 \times g$. The pellets were washed twice with 100 mM Tris-HCl (pH 7.5) before resuspending in 1 ml of the same buffer. The suspension was placed in an ice bath and sonicated for 1 min with Soniprep 150 Plus ultrasonic disintegrator (MSE). The lysate was centrifuged for 10 min at $10,000 \times g$ at 4°C and the supernatant was used in the assay. The reaction was started by adding 100 or 200 μ l of the crude extract to 0.9 or 0.8 ml of the reaction solution with following composition: 100 mM Tris-HCl (pH 7.5), 15 mM $MgCl_2$, 1 mM ADP, 10 mM phosphoenolpyruvate, 5.5 U of lactate dehydrogenase, and 0.1 mM NADH. NADH oxidation was determined by measuring the decrease in absorbance at 340 nm with a

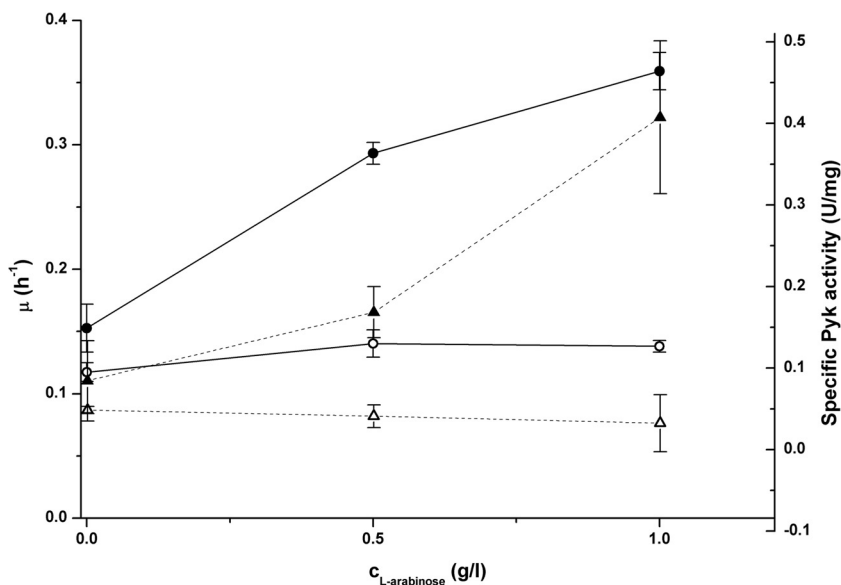


FIG 2 Effect of inducer (L-arabinose) concentration on growth rate (circles) and specific pyruvate kinase activity (triangles) of *pykF*-expressing cells (solid symbols) and plasmid control cells (open symbols). Error bars represent the standard deviations of three parallel cultivations.

UV-1601 UV-visible spectrophotometer (Shimadzu). NADH oxidation was also measured in a reaction solution lacking the substrate, phosphoenolpyruvate. This background activity was subtracted from the activity in the presence of the substrate. The reaction was carried out at room temperature, and a commercial preparation of pyruvate kinase was used as a positive control.

Medium optimization experiments and analysis. In order to optimize the cultivation medium for the maximal growth rate, the concentrations of gluconate and arabinose were varied according to the full factorial design. Three concentrations were examined for both variables, which resulted in nine combinations. Four replicated experiments were performed in the middle of the design space. Regression analysis was used to fit a quadratic model to the measured growth values. The model fit was reasonable with R^2 of 0.8502 and P value of 0.0185. The calculations were performed using a MATLAB software environment (24).

Metabolic flux balance analysis. The mechanisms behind improved growth rate were studied using a genome-scale metabolic model of *A. baylyi* ADP1 (25) and metabolic flux balance analysis (26). In practice, the maximal growth rate of *A. baylyi* ADP1 was predicted in aerobic conditions using gluconate or glucose as the sole carbon source. The maximal growth rate was predicted similarly both in the wild-type cell and in the *pykF*-expressing cell.

RESULTS

The functional expression of *pykF* in *A. baylyi* ADP1 leads to increased growth rate on gluconate. In order to enable pyruvate kinase activity in *A. baylyi* ADP1, the gene coding for the enzyme was cloned from *E. coli* K-12 MG1655 into an expression vector pBAV1C, derived from pBAV1k (27), as explained elsewhere (20), downstream of the arabinose promoter. This promoter was chosen because it allows the expression level of the *pykF* to be regulated by varying the arabinose concentration in the medium. In addition, the arabinose promoter has been shown to be functional in *A. baylyi* ADP1 (28).

The effect of *pykF* expression on growth rate was determined by precultivating the cells in the absence of the inducer and using it to start cultivations at a sodium-D-gluconate concentration of 20 g/liter and L-arabinose concentrations of 0, 0.5, or 1 g/liter

(Fig. 2). Increasing the inducer concentration elevated both the specific pyruvate kinase activity and the growth rate of the cells. When the inducer concentration was increased from 0 to 1 g/liter, the growth rate could be increased to an ~2.6-fold higher value, whereas the growth rate of the plasmid control cells remained at approximately the same level. A plating experiment was used to verify that the increase in OD achieved with *pykF* expression correlated with an increased number of CFU (data not shown).

Computational prediction of the metabolic flux redistribution caused by *pykF* expression was not able to explain the increased growth rate. The new *pykF* pathway was predicted to be in use in its full capacity, but the predicted growth rate increase was marginal. This contrast to the observed behavior is probably due to missing functionality in the model such as the lack of genetic regulation.

Optimization of *pykF* expression and substrate concentration. The D-gluconate concentration for initial characterization of the engineered cells was selected in arbitrary fashion, and the results presented above probably do not represent the most drastic effect generated by the *pykF* expression. In the optimization of growth rate, it was assumed that the difference in growth rates of wild-type cells and the engineered cells would depend mainly on the concentration of the substrate and *pykF* expression level. The regression model predicted the maximal growth of the engineered cells to be $0.44 h^{-1}$, which can be obtained using 4 and 15 g/liter of L-arabinose and sodium-D-gluconate, respectively. The model indicated that the growth rates would not be improved by continuing the optimization (data not shown).

***pykF* expression increases growth rate on gluconate without affecting biomass yield or substrate consumption and without significant overflow metabolite production.** *A. baylyi* ADP1 cells with the *pykF* expression plasmid or an empty plasmid were cultivated for 31 h under the optimized carbon source and inducer concentrations (Fig. 3). Both cell types grew to a similar biomass and consumed similar amounts of gluconate, but *pykF*-expressing cells reached stationary phase approximately twice as fast as the

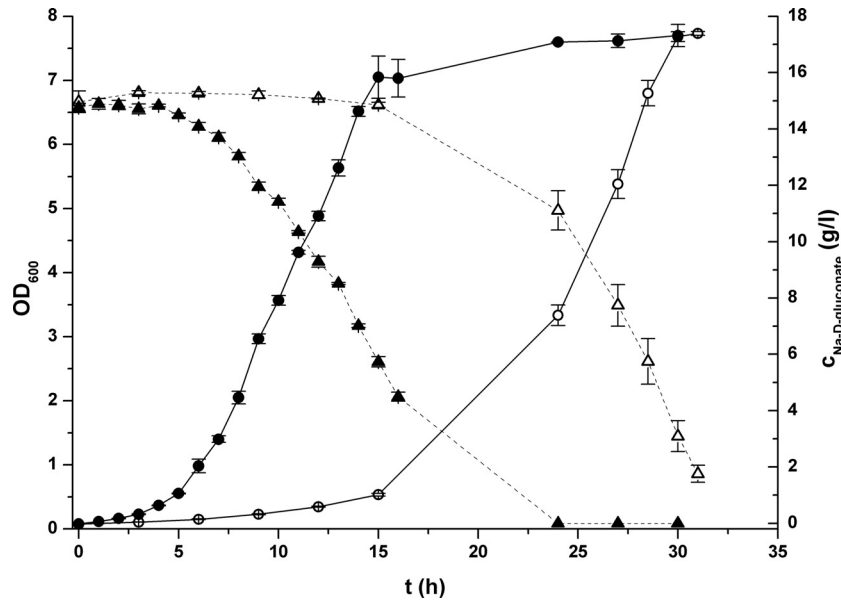


FIG 3 Growth (circles) and gluconate consumption (triangles) of engineered cells (solid symbols) and cells with an empty plasmid (open symbols). The cultivations were carried out in triplicate.

plasmid control cells. The growth rates at the beginning of the cultivations were $0.44 \pm 0.01 \text{ h}^{-1}$ for the engineered cells and $0.12 \pm 0.01 \text{ h}^{-1}$ for the plasmid control cells. The growth rates for the engineered cells were included in the statistical medium optimization.

In the plasmid control cell cultivations no overflow metabolites were detected. For the engineered cells, the only overflow metabolites detected with HPLC analysis were acetate and ethanol. Acetate concentration was above the detection level only transiently and remained below 1.0 mM. Ethanol was detected from the early part of the cultivations until the end of the experiment,

and its concentration remained at a level of approximately 1.0 to 1.5 mM. Since the concentrations of these compounds remained at very low levels, it can be assumed that the overflow metabolism should not cause similar problems as, for example, acetate accumulation causes with *E. coli*, which generally starts to produce acetate if the growth rate exceeds 0.2 h^{-1} (29).

Characterization of growth and wax ester production on glucose. Cells expressing *pykF* and cells with an empty plasmid were cultivated on glucose to show that the improvement in growth occurred also on this carbon source. Figure 4 shows that both strains had a lag phase of similar length. In the exponential phase

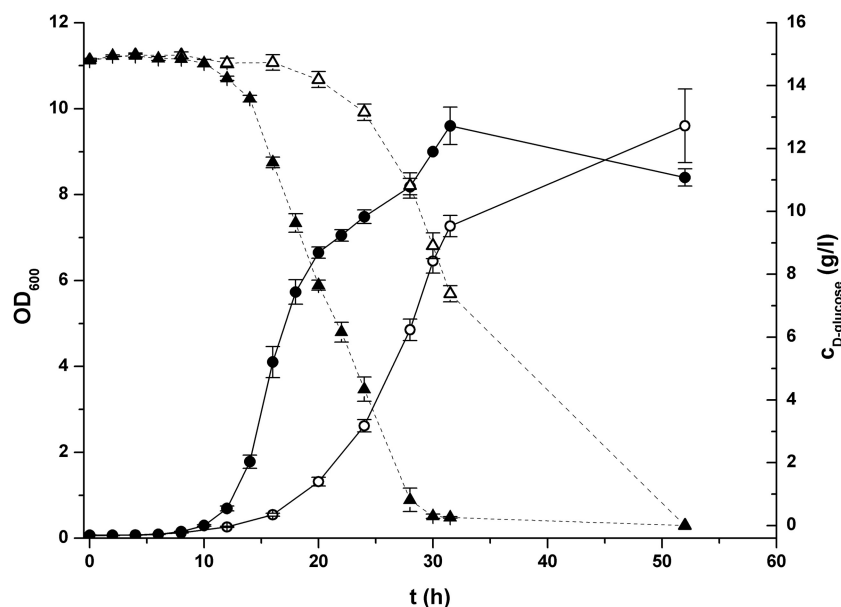


FIG 4 *pykF*-expressing cell (solid symbols) and plasmid control cell (open symbols) growth (spheres) and substrate consumption (triangles) on glucose. Both strains were cultivated in triplicates.

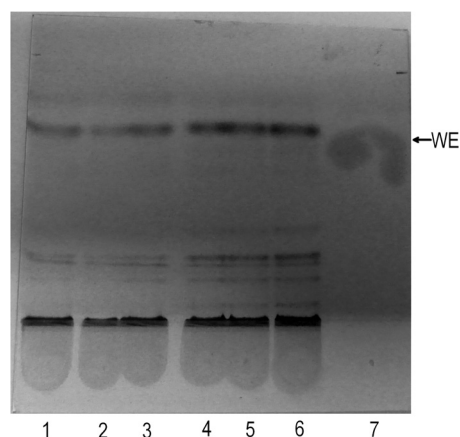


FIG 5 TLC analysis of wax ester production from glucose of plasmid control cells at 30 h (lanes 1 to 3) and *pykF*-expressing cells at 20 h (lanes 4 to 6) after the beginning of the cultivation. The lipids were extracted from same volume of triplicate cultivations of both cells and applied on the plate at volumes corresponding to same amount of biomass. A 1-mg portion of palmityl palmitate (lane 7) was used as a wax ester standard (WE).

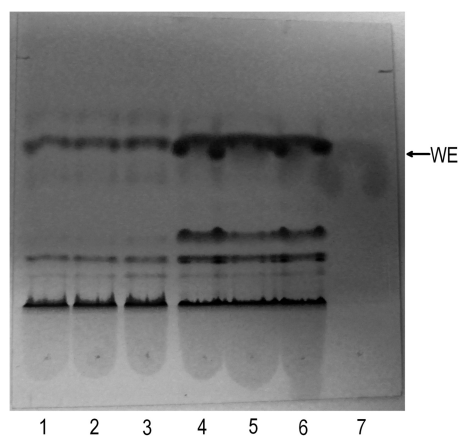


FIG 6 TLC analysis of wax ester production from glucose at 30 h after the beginning of the cultivations. Samples from cultivations of plasmid control cells (lanes 1 to 3) and *pykF*-expressing cells (lanes 4 to 6) were applied to the plate at identical volumes. The wax ester standard (WE) in lane 7 is as described for Fig. 5.

of growth, *pykF*-expressing cells grew with a specific growth rate of $0.42 \pm 0.01 \text{ h}^{-1}$ and plasmid control cells grew with a specific growth rate of $0.18 \pm 0.00 \text{ h}^{-1}$. Thus, there was no large difference between gluconate and glucose cultivations with respect to the growth rate of *pykF*-expressing cells, whereas plasmid control cells grew somewhat more rapidly on glucose. *pykF* expression did not affect substrate consumption, as was the case when gluconate was used as a carbon source. On the other hand, neither of the cells produced overflow metabolites during the cultivation on glucose.

Lipid extracts from *pykF*-expressing cells at 20 h and from plasmid control cells at 30 h after the beginning of the cultivations—time points at which both types of cells were in approximately the same phase of growth and had consumed similar amounts of glucose—were analyzed by TLC (Fig. 5). The samples were applied to the TLC plate so that differences in ODs were taken into account. The difference between bands for wax esters is rather small, but the wax ester production of *pykF*-expressing cells did not decrease with increased growth rate since they appeared to have accumulated slightly more of these storage lipids. In order to show that the increase in growth rate could be used to increase the wax ester yield relative to the cultivation time, samples acquired at 30 h after the beginning of the cultivations were analyzed by TLC (Fig. 6). At this time point, when *pykF*-expressing cells had consumed nearly all of the glucose, the engineered cells had accumulated drastically more wax esters compared to the plasmid control cells. The intense bands below the wax ester bands in the lanes for the *pykF*-expressing cell samples, which are very faint in the lanes of plasmid control cells, were not specific to the engineered cells, and they could be seen at similar intensities in samples of plasmid control cells acquired at 52 h after the beginning of the cultivations (data not shown).

DISCUSSION

A. baylyi ADP1's growth rate on gluconate could be increased in a controlled fashion by regulating expression level of *E. coli*'s gene for pyruvate kinase, *pykF*. The growth rates of wild-type ADP1 in our previous experiments (data not shown) have been in the same range as in glucose cultivations reported by Kaplan and Rosenberg

(glucose at 28 mM [5 g/liter]) (30) and van Schie et al. (glucose at 10 mM) (31). The strain from which *A. baylyi* ADP1 has been derived, BD4, has a doubling time on 28 mM glucose that is 0.6 times that of ADP1 and produces approximately twice as much extracellular rhamnose, a major sugar component of exopolysaccharides, as ADP1 (30). Here, we were able to increase ADP1's growth rate on gluconate to a value more than three times higher than that of control cells carrying an empty plasmid by inducing *pykF* expression, and on glucose the growth rate was more than doubled.

When grown to stationary phase on optimized gluconate and arabinose concentrations, the engineered cells showed an expected increase in growth rate. The doubling time of the engineered cells was 1.6 h, while plasmid control cells had a doubling time of 5.6 h. Furthermore, the amount of biomass formed and substrate consumption did not change with the increased growth rate. The expression of pyruvate kinase directs carbon flow from glucose degradation toward acetyl coenzyme A production which could be expected to trigger acetate accumulation. In *Bacillus subtilis* the removal of pyruvate kinase activity decreases acetate production and increases biomass yield on glucose (32). Also, the increased growth rate, or increased glucose consumption, causes *E. coli* to accumulate this overflow metabolite. However, we detected acetate only at very small concentrations in gluconate cultivations, and *pykF* expression did not greatly increase acetate production. Acetate is readily catabolized by *A. baylyi* ADP1, and its presence represses consumption of aromatic compounds (7). Thus, it might be that, if any acetate or some other organic acid is produced in small amounts during the cultivation, it is consumed rapidly and does not have time to accumulate in the medium. However, this might not be the case if a stronger promoter would have been used, but the results show that at optimized gluconate concentration and *pykF* expression level, overflow metabolites do not accumulate to any significant amount. It seems that organic acid accumulation should not cause similar problems with *A. baylyi* as it does with some other bacteria used in biotechnological applications, especially since all overflow metabolites were absent from the samples of glucose cultivations.

When glucose was used as a carbon source, an increase in growth rate of *pykF*-expressing cells similar to the one on gluconate was observed. On this carbon source the plasmid control cells grew somewhat faster than on gluconate and had a doubling time of ~3.8 h. The doubling time of the engineered cells was ~1.7 h, a value similar to the doubling time obtained on gluconate. This increase in growth rate could be applied to increasing the wax ester yield in the batch cultivation. After 30 h of cultivation, the *pykF*-expressing cells had accumulated much more of these storage lipids than the plasmid control cells. This is not unexpected, since it has been shown that wax ester production continues in the stationary phase in *A. baylyi* cultivations (33), and the engineered cells had had 10 h more time than did the plasmid control cells to consume glucose. This increase in wax ester content could have been simply due to the fact that more glucose was converted to it, and the relative wax ester yield from this substrate could have been decreased, which has been shown to occur with *A. baylyi* with increasing growth rates in nitrogen-limited cultivations (33). However, the samples acquired when both cells were in the late exponential phase, when both strains had consumed similar amount of glucose, showed that *pykF*-expressing cells' wax ester production had not decreased.

A. baylyi ADP1's growth rate could be successfully increased without major drawbacks by expressing *E. coli*'s gene for pyruvate kinase, thus reducing greatly the cultivation time needed to reach stationary phase on gluconate or glucose. This metabolic engineering approach was successfully applied in increasing wax ester production from glucose in a batch cultivation, but its suitability in production of other possible products, such as cyanophycin and exopolysaccharides with emulsifying activities, remains to be elucidated. The lack of any negative effects on the studied parameters indicate that this approach could be used in other biotechnological applications using glucose as a carbon source and *A. baylyi* as a host organism.

ACKNOWLEDGMENTS

This study was supported by the Jenny and Antti Wihuri Foundation and the Academy of Finland (grants 140018, 139830, and 272602).

REFERENCES

- Marr AG. 1991. Growth rate of *Escherichia coli*. Microbiol. Rev. 55:316–333.
- Chao Y-P, Patnaik R, Roof WD, Young RF, Liao JC. 1993. Control of gluconeogenic growth by *pps* and *pck* in *Escherichia coli*. J. Bacteriol. 175:6939–6944.
- Krajewski V, Simic P, Mouncey NJ, Bringer S, Sahn H, Bott M. 2010. Metabolic engineering of *Gluconobacter oxydans* for improved growth rate and growth yield on glucose by elimination of gluconate formation. Appl. Environ. Microbiol. 76:4369–4376. <http://dx.doi.org/10.1128/AEM.03022-09>.
- Juni E, Janik A. 1969. Transformation of *Acinetobacter calcoaceticus* (*Bacterium anitratum*). J. Bacteriol. 98:281–288.
- Young DM, Parke D, Ornston LN. 2005. Opportunities for genetic investigation afforded by *Acinetobacter baylyi*, a nutritionally versatile bacterial species that is highly competent for natural transformation. Annu. Rev. Microbiol. 59:519–551. <http://dx.doi.org/10.1146/annurev.micro.59.051905.105823>.
- Fewson CA. 1985. Growth yields and respiratory efficiency of *Acinetobacter calcoaceticus*. J. Gen. Microbiol. 131:865–872.
- Fischer R, Bleichrodt FS, Gerischer UC. 2008. Aromatic degradative pathways in *Acinetobacter baylyi* underlie carbon catabolite repression. Microbiology 154:3095–3103. <http://dx.doi.org/10.1099/mic.0.2008/016907-0>.
- de Berardinis V, Vallenet D, Castelli V, Besnard M, Pinet A, Cruaud C, Samair S, Lechaplais C, Gyapay G, Richez C, Durot M, Kreimeyer A, Le Fèvre F, Schächter V, Pezo V, Döring V, Scarpelli C, Médigue C, Cohen GN, Marlière P, Salanoubat M, Weissenbach J. 2008. A complete collection of single-gene deletion mutants of *Acinetobacter baylyi* ADP1. Mol. Syst. Biol. 4:174. <http://dx.doi.org/10.1038/msb.2008.10>.
- Abdel-El-Haleem D. 2003. *Acinetobacter*: environmental and biotechnological applications. Afr. J. Biotechnol. 2:71–74.
- Elbahloul Y, Steinbüchel A. 2006. Engineering the genotype of *Acinetobacter baylyi* sp. strain ADP1 to enhance biosynthesis of cyanophycin. Appl. Environ. Microbiol. 72:1410–1419. <http://dx.doi.org/10.1128/AEM.72.2.1410-1419.2006>.
- Shabtai Y, Gutnick DL. 1986. Enhanced emulsan production in mutants of *Acinetobacter calcoaceticus* RAG-1 selected for resistance to cetyltrimethylammonium bromide. Appl. Environ. Microbiol. 52:146–151.
- Santala S, Efimova E, Kivinen V, Larjo A, Aho T, Karp M, Santala V. 2011. Improved triacylglycerol production in *Acinetobacter baylyi* ADP1 by metabolic engineering. Microb. Cell. Fact. 10:36. <http://dx.doi.org/10.1186/1475-2859-10-36>.
- Pronk JT, Bakker AW, van Dam HE, Straathof AJJ, Scheffers WA, van Dijken JP. 1988. Preparation of D-xylulose from D-xylose. Enzyme Microb. Technol. 10:537–542. [http://dx.doi.org/10.1016/0141-0229\(88\)90046-4](http://dx.doi.org/10.1016/0141-0229(88)90046-4).
- Dolin MI, Juni E. 1978. Utilization of oxalacetate by *Acinetobacter calcoaceticus*: evidence for coupling between malic enzyme and malic dehydrogenase. J. Bacteriol. 133:786–793.
- Taylor WH, Juni E. 1961. Pathways for biosynthesis of a bacterial capsular polysaccharide. II. Carbohydrate metabolism and terminal oxidation mechanisms of a capsule-producing coccus. J. Bacteriol. 81:694–703.
- Sauer U, Eikmanns BJ. 2005. The PEP-pyruvate-oxaloacetate node as the switch point for carbon flux distribution in bacteria. FEMS Microbiol. Rev. 29:765–794. <http://dx.doi.org/10.1016/j.femsre.2004.11.002>.
- Liao JC, Chao Y-P, Patnaik R. 1994. Alteration of the biochemical valves in the central metabolism of *Escherichia coli*. Ann. N. Y. Acad. Sci. 745:21–34.
- Farmer WR, Liao JC. 1997. Reduction of aerobic acetate production by *Escherichia coli*. Appl. Environ. Microbiol. 63:3205–3210.
- Sambrook J, Fritsch EF, Maniatis T. 1990. Molecular cloning: a laboratory manual. Cold Spring Harbor Laboratory Press, Cold Spring Harbor, NY.
- Santala S, Efimova E, Koskinen P, Karp MT, Santala V. 2014. Rewiring the wax ester production pathway of *Acinetobacter baylyi* ADP1. ACS Synth. Biol. 3:145–151. <http://dx.doi.org/10.1021/sb4000788>.
- Metzgar D, Bacher JM, Pezo V, Reader J, Döring V, Schimmel P, Marlière P, de Crecy-Lagard V. 2004. *Acinetobacter* sp. ADP1: an ideal model organism for genetic analysis and genome engineering. Nucleic Acids Res. 32:5780–5790. <http://dx.doi.org/10.1093/nar/gkh881>.
- Santala S, Efimova E, Karp M, Santala V. 2011. Real-time monitoring of intracellular wax ester metabolism. Microb. Cell. Fact. 10:75. <http://dx.doi.org/10.1186/1475-2859-10-75>.
- Netzer R, Malgorzata K, Rittmann D, Peters-Wendisch PG, Eggeling L, Wendisch VF, Sahn H. 2004. Roles of pyruvate kinase and malic enzyme in *Corynebacterium glutamicum* for growth on carbon sources requiring gluconeogenesis. Arch. Microbiol. 182:354–363. <http://dx.doi.org/10.1007/s00203-004-0710-4>.
- MathWorks, Inc. 2011. MATLAB 7.13. MathWorks, Inc., Natick, MA.
- Durot M, Le Fèvre F, de Berardinis V, Kreimeyer A, Vallenet D, Combe C, Smidtas S, Salanoubat M, Weissenbach J, Schächter V. 2008. Iterative reconstruction of a global metabolic model of *Acinetobacter baylyi* ADP1 using high-throughput growth phenotype and gene essentiality data. BMC Syst. Biol. 2:85. <http://dx.doi.org/10.1186/1752-0509-2-85>.
- Fell DA, Small JR. 1986. Fat synthesis in adipose tissue: an examination of stoichiometric constraints. Biochem. J. 238:781–786.
- Bryksin AV, Matsumura I. 2010. Rational design of a plasmid origin that replicates efficiently in both Gram-positive and Gram-negative bacteria. PLoS One 5:e13244. <http://dx.doi.org/10.1371/journal.pone.0013244>.
- Murin CD, Segal K, Bryksin A, Matsumura I. 2012. Expression vectors for *Acinetobacter baylyi* ADP1. Appl. Environ. Microbiol. 78:280–283. <http://dx.doi.org/10.1128/AEM.05597-11>.
- Eiteman MA, Altman E. 2006. Overcoming acetate in *Escherichia coli* recombinant protein fermentations. Trends Biotechnol. 24:530–536. <http://dx.doi.org/10.1016/j.tibtech.2006.09.001>.

30. Kaplan N, Rosenberg E. 1982. Exopolysaccharide distribution of and bioemulsifier production by *Acinetobacter calcoaceticus* BD4 and BD413. *Appl. Environ. Microbiol.* **44**:1335–1341.
31. van Schie BJ, Rouwenhorst RJ, van Dijken JP, Kuenen JG. 1989. Selection of glucose-assimilating variants of *Acinetobacter calcoaceticus* LMD 79.41 in chemostat culture. *Antonie Van Leeuwenhoek* **55**:39–52. <http://dx.doi.org/10.1007/BF02309618>.
32. Fry B, Zhu T, Domach MM, Koepsel RR, Phalakornkule C, Atai MM. 2000. Characterization of growth and acid formation in a *Bacillus subtilis* pyruvate kinase mutant. *Appl. Environ. Microbiol.* **66**:4045–4049. <http://dx.doi.org/10.1128/AEM.66.9.4045-4049.2000>.
33. Fixter LM, Nagi MN, McCormack JG, Fewson CA. 1986. Structure, distribution, and function of wax esters in *Acinetobacter calcoaceticus*. *J. Gen. Microbiol.* **132**:3147–3157.